

## A CFD Investigation of Emissions Formation in HCCI Engines, Including Detailed NO<sub>x</sub> Chemistry

E.H. Kung, S. Priyadarshi, B.C. Nese and D.C. Haworth

The Pennsylvania State University, University Park, PA 16802

### Abstract

Three-dimensional time-dependent CFD simulations of autoignition and emissions are reported for an idealized engine configuration under HCCI-like operating conditions. The emphasis is on NO<sub>x</sub> emissions. Detailed NO<sub>x</sub> chemistry is integrated with skeletal autoignition mechanisms for n-heptane and iso-octane fuels. A storage/retrieval scheme is used to accelerate the computation of chemical source terms, and turbulence/chemistry interactions are treated using a transported probability density function (PDF) method. Simulations include direct in-cylinder fuel injection, and feature direct coupling between the stochastic Lagrangian fuel-spray model and the gas-phase stochastic Lagrangian PDF method. For the conditions simulated, consideration of turbulence/chemistry interactions is essential. Simulations that ignore these interactions fail to capture global heat release and ignition timing, in addition to emissions. For these lean, low-temperature operating conditions, engine-out NO<sub>x</sub> levels are low and NO<sub>x</sub> pathways other than thermal NO are dominant. Engine-out NO<sub>2</sub> levels exceed engine-out NO levels in some cases. In-cylinder inhomogeneity and unmixedness must be considered for accurate emissions predictions. These findings are consistent with results that have been reported recently in the HCCI engine literature.

### 1. Introduction

Homogenous-charge compression-ignition (HCCI) and related quasi-homogeneous low-temperature combustion systems have been receiving considerable attention in recent years [1, 2]. Such systems offer the potential for high thermal efficiency with low engine-out NO<sub>x</sub> and soot emissions, and can be designed to burn a variety of fuels including conventional gasolines and diesel fuels. Detailed chemical mechanisms are required to capture autoignition, and NO<sub>x</sub> pathways other than thermal NO must be considered at the lean, low-temperature conditions that characterize HCCI combustion. Zonal models [3] and hybrid CFD/zonal models [4] are appropriate when flow/chemistry interactions are weak (e.g., robust autoignition of nearly homogeneous reactants), but detailed-chemistry CFD and explicit accounting for turbulence/chemistry interactions are required for less robust operating conditions, stronger departures from homogeneity (e.g., relatively late in-cylinder fuel injection), and accurate emissions predictions [5].

By design, HCCI engine-out NO<sub>x</sub> should be low (10's of ppm or lower). NO<sub>x</sub> prediction remains an issue because of the cost and complexity of after-treatment systems for low-temperature, oxygen-rich exhaust streams and because of the need to characterize marginal and transitional operating conditions. It has been suggested that the N<sub>2</sub>O pathway may be dominant under some HCCI operating conditions [6]. Relatively high levels of engine-out NO<sub>2</sub>, in some cases exceeding NO, have been reported in some HCCI engine experiments [7]. And it has been shown that temperature and composition inhomogeneities and/or unmixedness have a strong influence on NO<sub>x</sub> levels [7, 8].

We have been working to develop CFD-based methods that accommodate detailed thermochemistry and turbulence/chemistry interactions, while remaining computationally practicable. The essential elements are chemical mechanisms (developed elsewhere), a consistent hybrid particle/finite-volume composition probability density function (PDF) method, and storage/retrieval-based chemistry acceleration. Embouazza, Haworth and Darabiha [9] implemented Pope's *in situ* adaptive tabulation (ISAT) method [10] in multidimensional CFD calculations of HCCI autoignition, and reported results for n-heptane/air mechanisms containing up to 160 species and 1,540 reactions. An ISAT-based algorithm, DOLFA (Database for On-Line Function Approximation [11]), has been developed for highly nonstationary combustion processes, such as those that occur in reciprocating-piston IC engines. Consistent hybrid particle/finite-volume PDF algorithms have been developed for three-dimensional unsteady flows on unstructured, deforming computational meshes [12]. And these methods have been integrated and applied to investigations

Table 1: Engine configuration and operating conditions for two fuels. In all cases the bore diameter is 82.55 mm, TDC clearance is 10.0 mm, engine speed is 1000 r/min, and there is a 0.5 mm radial  $\times$  5 mm axial piston top-ring-land-crevice ( $\sim$ 1.2% of TDC volume).

N-heptane	Stroke	150 mm
	Compression ratio	15.8:1
	Fueling	34% premixed; 66% direct in-cylinder injection, 90-75° BTDC
	Equivalence ratio/EGR	0.24/0%
	Intake-valve-closing (IVC) swirl/tumble ratios	1.5/0.75
	IVC $p$ & $T$ ; piston/liner $T$ 's	1 atm & 320 K; 450 K/400 K
Iso-octane	Stroke	145 mm
	Compression ratio	15.3:1
	Fueling	Direct in-cylinder injection, 175-160° BTDC
	Equivalence ratio/EGR	0.24/ $\sim$ 2% by mass
	Intake-valve-closing (IVC) swirl/tumble ratios	1.0/0.5
	Case A: IVC $p$ & $T$ ; piston/liner $T$ 's	1 atm & 450 K; 450 K/425 K
	Case B: IVC $p$ & $T$ ; piston/liner $T$ 's	1 atm & 430 K; 450 K/400 K

of autoignition and emissions in HCCI engines [5]. Using these high-end models, it has been shown that turbulence and turbulence/chemistry interactions always have a strong influence on computed emissions; in cases with strong in-cylinder flow, high departures from spatial homogeneity, and/or marginal operating conditions, they influence the global combustion event (i.e., ignition timing) as well. Other issues have been addressed, including the influence of model coefficients on computed results [13] and the importance of simulating multiple engine cycles to ensure that a statistically stationary state has been reached [14]. The models and algorithms are being refined as we continue to gain experience with their effective use for engine simulations.

In this paper, we report recent CFD simulations for direct-injection engines operating in HCCI or quasi-HCCI combustion modes using n-heptane and iso-octane fuels. The emphasis is on NOx emissions.

## 2. Physical Models and Numerical Methods

Three-dimensional, time-dependent Reynolds-averaged simulations have been performed using an unstructured, deforming-mesh, compressible finite-volume CFD solver. A Lagrangian particle Monte Carlo method has been implemented to solve the modeled composition PDF transport equation using a consistent hybrid particle/finite-volume method [12], thereby explicitly accounting for turbulent fluctuations in composition and enthalpy (temperature) about the local cell-mean values. A standard gradient transport approximation has been used together with a two-equation  $k - \epsilon$  turbulence model to account for transport by turbulent velocity fluctuations, and a simple pair-exchange model has been used for molecular mixing [15].

Thermochemistry has been implemented using the CHEMKIN libraries [16]. Two chemical mechanisms have been used: an n-heptane mechanism based on a 40-species skeletal mechanism from Chalmers and the University of Wisconsin [17, 18] and an iso-octane mechanism based on the 79-species skeletal mechanism of Ogink and Golovitchev [19, 20]. In both cases, Glarborg's NOx chemistry [21] has been integrated into the underlying oxidation mechanism. The integrated n-heptane/NOx mechanism has 70 species and 376 reactions, and the integrated iso-octane/NOx mechanism has 105 species and 608 reactions. It has been verified through zero-dimensional simulations that the NOx chemistry has negligible influence on computed ignition delays, temperature, and major species. DOLFA [11] has been used to reduce the computational overhead of these large (for multidimensional CFD) chemical mechanisms.

Direct in-cylinder liquid fuel injection has been modeled using stochastic Lagrangian models that are based on the KIVA spray formulation [22, 23]. A novel feature of the present simulations is the coupling between the Lagrangian parcel spray model and the gas-phase particle PDF method. As spray parcels evaporate in accordance with the spray vaporization model, new PDF notional particles are introduced at the exact location of each vaporizing parcel with the correct mass, composition (pure fuel), and temperature. This captures in a natural and direct manner the high levels of local gas-phase concentration and temperature fluctuations that arise from spray vaporization. This effect must be modeled in more conventional approaches, and usually is ignored [24, 25].

To isolate the roles of inhomogeneities and unmixedness, results from three levels of modeling are compared: a zero-dimensional adiabatic model ("0D adiabatic"), a CFD-based model without consideration of turbulence/chemistry interactions ("CFD wo/PDF"), and a CFD-based model with consideration of turbulence/chemistry interactions using a transported PDF method ("CFD w/PDF"). In general, 0D adiabatic models predict advanced ignition, a high rate

Table 2: Global results for n-heptane. Emissions are global in-cylinder mole fractions at 30° ATDC, and UHC excludes the fuel.

Model	$CA_{p\ max}$ [°ATDC]	$(dp/d\theta)_{max}$ [bar/CA°]	CO [ppm]	Fuel [ppm]	UHC [ppm]	NO [ppm]	NO <sub>2</sub> [ppm]
CFD wo/PDF	5.6	8.4	9000	20	2684	0.000013	0.00055
CFD w/PDF	5.5	4.5	4547	20	1500	0.62	0.87

Table 3: Global results for iso-octane. 0D adiabatic emissions are mole fractions at BDC expansion, CFD emissions are global in-cylinder mole fractions at 30° ATDC, and UHC excludes the fuel.

Case	Model	$CA_{p\ max}$ [°ATDC]	$(dp/d\theta)_{max}$ [bar/CA°]	CO [ppm]	Fuel [ppm]	UHC [ppm]	NO [ppm]	NO <sub>2</sub> [ppm]
A	0D adiabatic	0.0	28.2	0.049	0	0.043	7.9	0.70
	CFD wo/PDF	4.0	7.1	163	18	157	0.33	0.025
	CFD w/PDF	3.2	4.9	354	25	167	2.4	0.19
B	0D adiabatic	0.0	17.6	0.036	0	0.026	1.5	0.26
	CFD wo/PDF	14.8	1.4	1548	595	660	0.032	0.017
	CFD w/PDF	10.0	1.3	2433	39	438	0.19	0.044

of pressure rise, and low unburned hydrocarbon and CO emissions compared to higher-order models or experiments. CFD without turbulence/chemistry interactions (CFD wo/PDF) captures mean flow effects, wall heat transfer, and inhomogeneities in the mean fields; CFD with turbulence/chemistry interactions (CFD w/PDF) captures the effects of turbulent fluctuations about the local mean, in addition.

### 3. Engine Configuration and Operating Conditions

A simple pancake-chamber engine (flat head and piston) is simulated, including a piston top-ring-land crevice. The importance of the top-ring-land crevice in determining unburned hydrocarbon and CO emissions has been highlighted in a number of experimental [26] and modeling [5, 27] studies. Simulations begin at piston bottom-dead-center and are carried part-way through expansion with all valves closed. Further information is provided in Table 1. These correspond to low-speed, light-load operating conditions.

For n-heptane, multidimensional CFD results without (CFD wo/PDF), and with (CFD w/PDF) consideration of turbulence/chemistry interactions are compared for a single operating condition. A portion of the fuel is premixed while the remainder is injected directly into the combustion chamber over 15 crankangle degrees, starting 90 degrees before piston top-dead-center, using a centrally mounted fuel injector that sprays directly toward the piston.

Results from three levels of modeling (0D adiabatic, CFD wo/PDF, and CFD w/PDF) are compared for iso-octane. Two iso-octane cases are simulated that differ only in initial temperature (different by 20 K) and wall temperature (different by 25 K; wall temperature is not relevant for 0D adiabatic modeling). Fuel is injected over 15 crankangle degrees starting shortly after piston bottom-dead-center, again using a centrally mounted fuel injector that sprays directly toward the piston.

## 4. Results

Global results are reported in Tables 2 and 3 for n-heptane and iso-octane, respectively.

### 4.1. Pressure, Temperature, and Heat Release

The n-heptane case exhibits advanced ignition ( $CA_{p\ max} \approx 5.5^\circ\text{ATDC}$ , for CFD w/PDF) compared to ideal combustion phasing; in general, autoignition occurs somewhat early for n-heptane in HCCI-like combustion modes. Consideration of turbulence/chemistry interactions generally advances the ignition and broadens the heat-release event, resulting in lower peak rates of pressure rise,  $(dp/d\theta)_{max}$ . This behavior is evident in Table 2 and Figure 1.

Evidence of in-cylinder temperature inhomogeneity and unmixedness is provided in Figure 2. The peak difference between the maximum finite-volume cell temperature and the global volume-averaged in-cylinder temperature (a measure of inhomogeneity in the mean temperature field) exceeds 150 K for CFD wo/PDF, and is even larger (over 500 K) for CFD w/PDF. For CFD w/PDF, differences among individual particle temperatures within each finite-volume cell are indications of unmixedness. Figure 2 shows that there are particles whose temperature exceeds 2000 K when

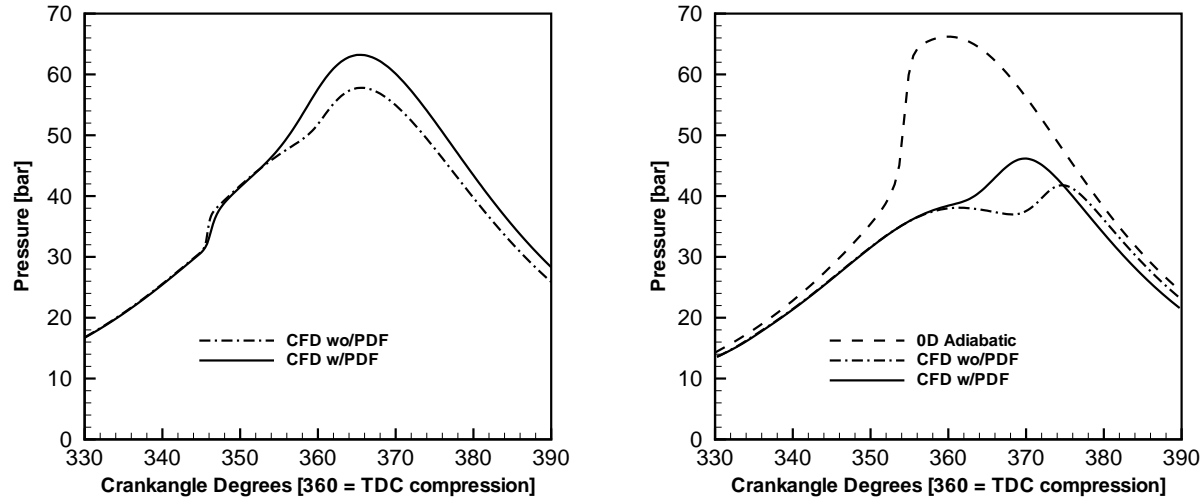


Fig. 1: Computed in-cylinder pressure versus crankangle. Left: n-heptane with two levels of modeling. Right: iso-octane Case B with three levels of modeling.

the global volume-averaged temperature and maximum finite-volume cell mean temperature both are below 1000 K. These large excursions in local temperatures from the volume-averaged temperature have a profound influence on emissions, in particular.

Iso-octane Case B exhibits satisfactory HCCI combustion phasing (peak pressure at  $10^\circ$  ATDC, for CFD w/PDF) while Case A (higher initial and wall temperature) ignites somewhat early (peak pressure at  $3.2^\circ$  ATDC). The peak rate of pressure rise from the 0D adiabatic model is excessive. Consideration of turbulence/chemistry interactions broadens the heat-release event, resulting in lower peak rates of pressure rise,  $(dp/d\theta)_{max}$ . Figure 1 shows dramatic differences among the computed pressure traces for the three levels of modeling.

#### 4.2. Emissions

In-cylinder levels of CO, unburned hydrocarbons excluding fuel (UHC), unburned fuel, NO, and NO<sub>2</sub> early in the expansion stroke are summarized in Tables 2 and 3. By this time CO, UHC, and fuel mole fractions are close to their engine-out frozen values while NO and NO<sub>2</sub> are still evolving (see below).

The strong influence of inhomogeneities and/or unmixedness on HCCI emissions that has been noted in earlier experimental and modeling studies [5, 7, 8] is evident in Tables 2 and 3. CFD emissions with versus without turbulence/chemistry interactions differ dramatically, and cannot be explained by the change in ignition timing alone. CO, UHC, and unburned fuel emissions are virtually zero from the 0D adiabatic model. All increase significantly with consideration of mean flow effects, wall heat transfer, and inhomogeneities in the mean fields (CFD wo/PDF). CO and UHC emissions can be higher or lower with consideration of turbulence/chemistry interactions (CFD w/PDF), depending on the operating conditions.

The NO<sub>x</sub> results are particularly interesting. For the conditions simulated, NO<sub>x</sub> levels are low, consistent with experimental measurements under similar conditions [7]. NO levels from the 0D adiabatic model are high compared to CFD wo/PDF values by virtue of the unrealistically high in-cylinder temperatures given by the 0D adiabatic model. NO and NO<sub>2</sub> levels with turbulence/chemistry interactions (CFD w/PDF) are at least one order of magnitude higher than those without turbulence/chemistry interactions (CFD wo/PDF). The computed time evolution of global in-cylinder NO, NO<sub>2</sub>, and N<sub>2</sub>O for n-heptane is plotted in Figure 3. For CFD w/PDF, N<sub>2</sub>O appears first, is consumed to generate NO, and NO in turn is consumed early during expansion to generate NO<sub>2</sub>. In this case, NO<sub>2</sub> exceeds NO by  $30^\circ$  ATDC, and the NO<sub>2</sub>/NO ratio continues to increase through the remainder of expansion (not shown). This is consistent with the suggestion that the N<sub>2</sub>O pathway is dominant under some HCCI operating conditions [6], as has been reported earlier in low-temperature, high-pressure, lean-premixed-flame calculations [28]. It also is consistent with the relatively high engine-out NO<sub>2</sub>/NO ratios that have been reported in the literature for some HCCI operating conditions [7]. In general, the modeling results support the conclusion that proper accounting of turbulence/chemistry interactions is essential to capture the relatively high NO<sub>2</sub>/NO ratios [7, 8] and other emissions.

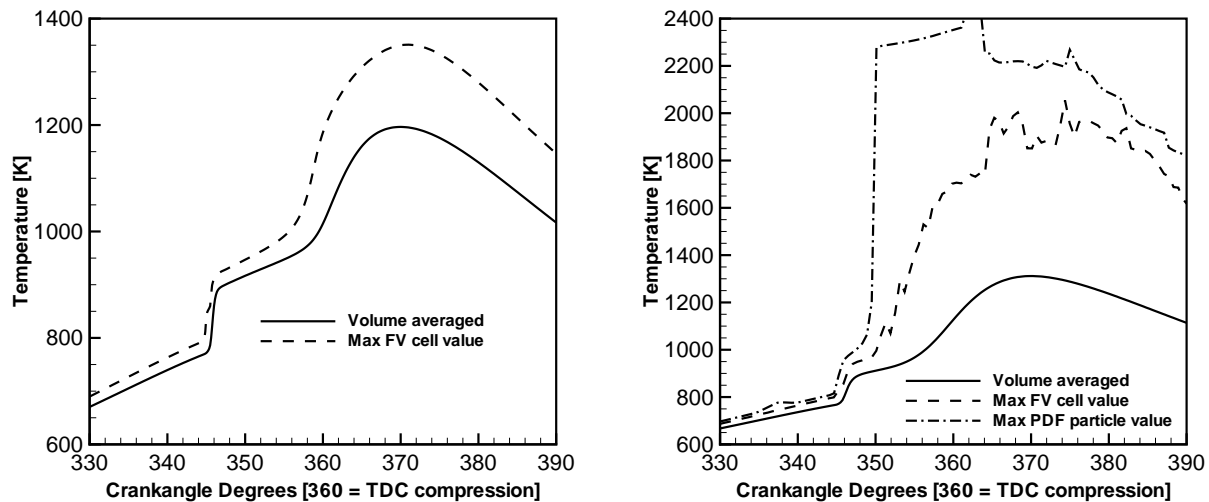


Fig. 2: Computed in-cylinder temperatures versus crankangle for n-heptane. Left: Volume-averaged in-cylinder temperature and maximum finite-volume cell mean temperature for CFD w/o/PDF. Right: Volume-averaged in-cylinder temperature, maximum finite-volume cell mean temperature, and maximum PDF notional particle temperature for CFD w/PDF.

## 5. Concluding remarks

The importance of turbulence/chemistry interactions on the global ignition event and emissions in HCCI engines has been demonstrated using multidimensional simulations. For these lean, low-temperature operating conditions, engine-out NO<sub>x</sub> levels are low, NO<sub>x</sub> pathways other than thermal NO are dominant, engine-out NO<sub>2</sub>/NO ratios are high, and in-cylinder inhomogeneity and unmixedness must be considered for accurate emissions predictions. These findings are consistent with other results that have been reported recently in the HCCI engine literature.

## Acknowledgments

This research has been supported by the National Science Foundation (grants CTS-0121573 and DGE-0338240), by the Department of Energy (grants DE-FC04-02AL67612 and DE-FC25-04NT42233), by the GM R&D Center, and by CD-adapco.

## References

- [1] F. Zhao, T.W. Asmus, D.N. Assanis, J.E. Dec, J.A. Eng and P.M. Najt (Eds.) 2003 *Homogeneous Charge Compression Ignition (HCCI) Engines: Key Research and Development Issues*. SAE International, Warrendale, PA.
- [2] M.C. Drake and D.C. Haworth 2006 Advanced gasoline engine development using optical diagnostics and numerical modeling. *Proc. Combust. Inst.* 31. To appear.
- [3] S.B. Fiveland and D.N. Assanis 2001 *SAE Paper No. 2001-01-1028*.
- [4] S.M. Aceves, D.L. Flowers, F. Espinosa-Loza, A. Babajimopoulos and D.N. Assanis 2005 *SAE Paper No. 2005-01-0115*.
- [5] Y.Z. Zhang, E.H. Kung and D.C. Haworth 2005 *Proc. Combust. Inst.* 30:2763-2771.
- [6] P. Mehresh, J. Souder, D. Flowers, U. Riedel and R.W. Dibble 2005 *Proc. Combust. Inst.* 30:2701-2709.
- [7] P. Amnéus, F. Mauss, M. Kraft, A. Vressner and B. Johansson 2005 *SAE Paper No. 2005-01-0126*.
- [8] J.W. Girard, R.W. Dibble, D.L. Flowers and S.M. Aceves 2002 *SAE Paper No. 2002-01-1758*.
- [9] M. Embouazza, D.C. Haworth and N. Darabiha 2002 *SAE Paper No. 2002-01-2773*.
- [10] S.B. Pope 1997 *Combust. Theory Modell.* 1:41-63.
- [11] I. Veljkovic, P. Plassmann and D.C. Haworth 2003 *Computational Science and Its Applications - ICCSA 2003, Lecture Notes in Computer Science (LNCS 2667), Part I*, pp. 643-653, Springer Verlag.
- [12] Y.Z. Zhang and D.C. Haworth 2004 *J. Comput. Phys* 194:156-193.
- [13] Y.Z. Zhang, E.H. Kung and D.C. Haworth 2005 PDF-based modeling of HCCI engine combustion. *2005 Joint Meeting of the U.S. Sections of the Combustion Institute*, Philadelphia, PA, 20-23 March 2005.
- [14] E.H. Kung, Y.Z. Zhang and D.C. Haworth 2005 A CFD study of the effects of internal EGR on ignition and emissions in HCCI engines. *2005 Joint Meeting of the U.S. Sections of the Combustion Institute*, Philadelphia, PA, 20-23 March 2005.
- [15] S. Subramaniam and D.C. Haworth 2000 *Internl. J. Engine Res.* 1:171-190.
- [16] R.J. Kee, F.M. Rupley and J.A. Miller 1989 *Sandia National Laboratories Report No. SAND89-8009B*.
- [17] V.I. Golovitchev 2000 <http://www.tfd.chalmers.se/valeri/MECH.html>. Chalmers University of Technology, Gothenburg, Sweden.
- [18] A. Patel, S.-C. Kong and R.D. Reitz 2004 *SAE Paper No. 2004-01-0558*.

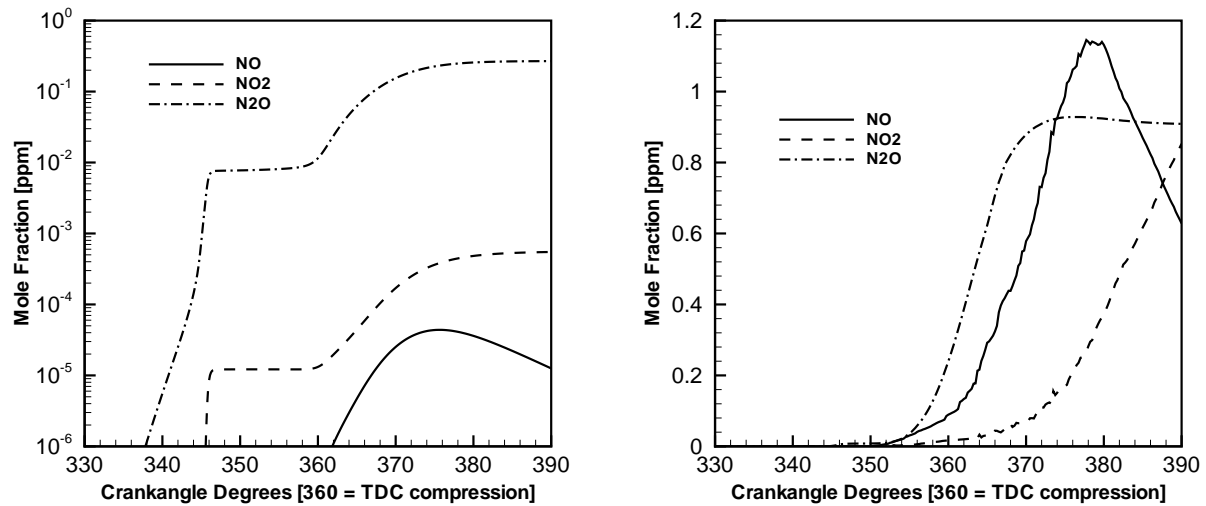


Fig. 3: Computed in-cylinder NO, NO<sub>2</sub>, and N<sub>2</sub>O mole fractions versus crankangle for n-heptane. Left: CFD w/o/PDF. Right: CFD w/PDF. Note the difference in the ordinate scales for the two figures.

- [19] R. Ogink and R. Golovitchev 2001 *SAE Paper No. 2001-01-3614*.
- [20] S.C. Kong, R.D. Reitz, M. Christensen and B. Johansson 2003 *SAE Paper No. 2003-01-1088*.
- [21] P. Glarborg, M.U. Alzueta, K. Dam-Johansen and J.A. Miller 1990 *Combust. Flame* 115:1-27.
- [22] A.A. Amsden, P.J. O'Rourke and T.D. Butler 1989 *Los Alamos National Laboratory Technical Report No. LA-11560-MS*.
- [23] A.M. Lippert, S.M. Chang, S. Are and D.P. Schmidt 2005 *SAE Paper No. 2005-01-0207*.
- [24] J. Réveillon and L. Vervisch 1998 *Proc. 1998 Summer Program of the Center for Turbulence Research*, Stanford University, Stanford, CA, pp.25-38.
- [25] J. Réveillon and L. Vervisch 2005 *J. Fluid Mech.* 537:317-347.
- [26] M. Christensen, A. Hultqvist and B. Johansson 2001 *SAE Paper No. 2001-01-1893*.
- [27] S.M. Aceves, D.L. Flowers, F. Espinosa-Loza, J. Martinez-Frias, R.W. Dibble, M. Christensen, B. Johansson and R.P. Hessel 2002 *SAE Paper No. 2002-01-2869*.
- [28] M.C. Drake and R.J. Blint 1991 *Combust. Sci. Technol.* 75:261-285.